World Conference on Timber Engineering Oslo 2023

EXPERIMENTAL AND NUMERICAL ANALYSES OF A CONNECTION FOR CLT STRUCTURES

Lars Blomqvist[1] , Roberto Crocetti[2], August Claesson[3], Zakaria Ben Osmane[4], Rune Ziethén[5], Marie Johansson[6]

ABSTRACT: Although building systems made of cross-laminated timber (CLT) have become common in Sweden in the past 20 years and they have developed rapidly during the same period, steps remain to be taken to simplify the assembly of such systems, especially at construction sites. Current construction methods, however, remain labour-intensive and thus show room for improvement.

This paper describes a novel connection for the assembly of building elements made of CLT. Simple and inexpensive, the connection is fairly insensitive to manufacturing tolerances and enables rapid, more efficient construction than the connections for CLT structures currently used. Test results show the excellent strength and stiffness of the connection, which also allows the replacement of numerous fasteners, including nails and screws, with only a single steel rod.

KEYWORDS: assembly, connections, cross-laminated timber

1 INTRODUCTION

The deficit of affordable housing in Northern Europe requires the rate of housing production to increase in parallel to a decrease in production costs. Beyond that, construction needs to be more resource-efficient and, as such, more environmentally friendly.

The construction of residential timber buildings with different structural systems has recently increased significantly in Europe. In Sweden, the development of structural systems for timber buildings has taken two paths: one driven by the single-family house industry with industrially built volume elements (i.e. also used for multi-storey buildings) and one driven by manufacturers of engineered wood products such as glulam and cross-laminated timber (CLT).

In CLT's case, the building method is well-suited for traditional construction industries, primarily due to its similarity to the building method used in prefabricated concrete. In Sweden, buildings made of CLT began being built approximately 20 years ago. In that context, the manufacture of CLT has recently shown significant intensification, with several production plants being launched in the past few years. Although CLT construction systems have developed rapidly during those years, steps remain to be taken to simplify the assembly of the CLT elements, especially at construction sites.

This paper reports the development of a connection for the assembly of building elements made of CLT. The proposed connection provides greater precision and enables a faster, more efficient process than typical connections used today. We have already reported a feasibility study [1] which, among other things, revealed how the inspiration of the presented connection comes from the furniture industry.

2 MATERIALS AND METHODS

The tested specimens were cut from five CLT panels of Norway spruce (*Picea abies* L.) into a nominal thickness of 120 mm. The panels were produced with five laminations with a C24 strength class. Regarding thickness, the two outer layers were 30 mm, while the three inner layers were 20 mm. The layers were bonded with a polyurethane reactive adhesive free of urea-formaldehyde, for a bonding that complied with EN 14080, type 1, according to EN 15425. Meanwhile, the density of the panels was in the range of 457–510 kg/cm^3. The two outer layers and the central layer had their grains oriented in the direction perpendicular to the load,

[1] Lars Blomqvist, RISE Research Institutes of Sweden, Sweden, lars.blomqvist@ri.se
[2] Roberto Crocetti, KTH Royal Institute of Technology, Sweden, crocetti@kth.se
[3] August Claesson, KTH Royal Institute of Technology, Sweden, august.claesson@hotmail.com
[4] Zakaria Ben Osmane, KTH Royal Institute of Technology, Sweden, zakariyabenosmane@yahoo.com
[5] Rune Ziethén, RISE Research Institutes of Sweden, Sweden, rune.ziethen@ri.se
[6] Marie Johansson, RISE Research Institutes of Sweden, Sweden, marie.johansson@ri.se

https://doi.org/10.52202/069179-0158

whereas the other two layers were oriented in the direction of the applied load. Last, the laminations were finger-jointed lengthwise but not edge-bonded.

Our study was performed on connections with varying geometries (see Figure 1a and Table 1), chiefly to assess the strength and stiffness of the proposed connection by varying two parameters: distance to end grain (DY) and lateral width (DX).

Altogether, seven specimen types were investigated experimentally, analytically and numerically. Two to three laboratory test repetitions on nominally identical specimens were performed in order to achieve satisfactory statistical relevance, which resulted in a total of 18 tested specimens.

Before commencing the laboratory tests, simplified hand calculations were performed in order to gain an approximate estimation of possible failure modes and corresponding failure load.

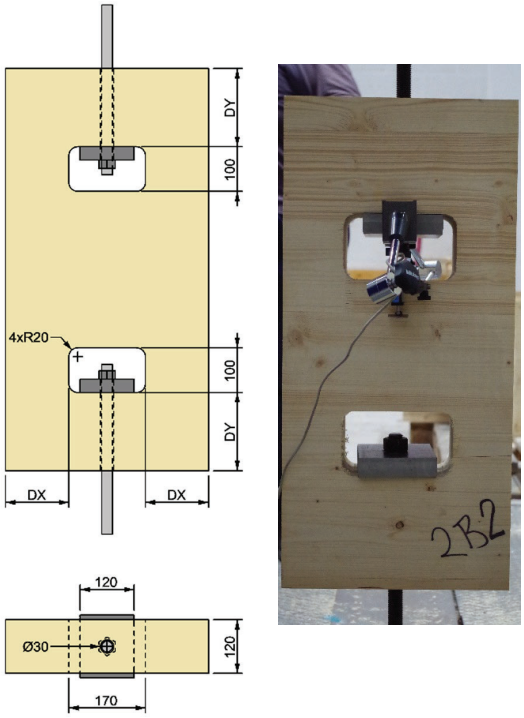

a b

Figure 1: *a) Dimensions of test samples*
b) Test set-up

Table 1: *Dimensions that varied in the samples by group*

Specimen group	DX (mm)	DY (mm)	Quantity (pcs)
1	90	100	3
2	165	100	3
3	90	175	3
4	238	175	3
5	90	250	2
6	155	250	2
7	238	250	2

Specimens were tested in a universal testing machine, and loads and corresponding displacement were recorded during the laboratory tests. The tensile axial load was applied to the specimens through a pair of steel rods 24 mm in diameter that were inserted in holes with a 30 mm diameter vertically drilled into the upper and lower parts of the specimens. The rods were fixed to the specimens by means of rectangular anchoring steel plates with a bearing area of 120 × 120 mm^2 and nuts at the end of the rods. The anchoring plates were allocated in openings made in the specimens that were rectangular in shape and had rounded off corners (Figure 1). Local displacements were measured using linear variable differential transducers (LVDT) placed directly above or directly below the rod's anchoring plate at each opening (Figure 1b). To avoid possible damage, the LVDTs were removed from the specimens when the load was approaching the predicted failure load of the connection.

2.1 The numerical model

Every specimen type was subjected to FE modelling with the commercial software Abaqus. The gap between the laminations within each layer was created by extruding a cut 0.01 mm wide. For each model, only half of the sample was modelled explicitly, and symmetry boundary conditions were used to represent the other half. All models used linear 8-noded brick elements with reduced integration and hourglass control. For groups 1, 3 and 5 of specimens, the FE mesh size was set to 6 mm.

The elastic material properties were the same for all models and are shown in Table 2. The properties are based on ones previously published [2]. For each layer, Direction 1 was oriented parallel to grain, Direction 2 was oriented in the direction perpendicular to the grain, and Direction 3 was set to point out of the plane of the panel.

Table 2: *Material properties, with E_i, υ_{ij} and G_{ij} indicating Young's modulus, Poisson's ratio and the shear modulus, respectively, in Directions 1, 2 and 3*

Name of the mechanical property	Numerical value
E_1	12,000 MPa
E_2	500 MPa
E_3	500 MPa
υ_{12}	0.3
υ_{13}	0.3
υ_{23}	0.3
G_{12}	600 MPa
G_{13}	600 MPa
G_{23}	60 MPa

The load was applied to the rod by using a reference point with a rigid body constraint, which allowed the load to be more evenly distributed over the end face of the rod. The load was modelled as a concentrated force acting on the reference point, its magnitude was set to the max load for each sample, and it was applied incrementally.

The boundary conditions used were different symmetry conditions applied to the symmetry surface of each sample.

https://doi.org/10.52202/069179-0158

The glued interaction between the layers of the CLT was handled by using a cohesive contact condition implemented in the FE software. Following past investigations [2], the bonded connection was given a stiffness of 1000 N/mm^3 in every direction; that condition was applied to all flat face surfaces of CLT, and no interaction between the lamination edges was used. The contact area between the steel anchor plate and the CLT was also simulated by using a special contact condition with hard contact typically for the surfaces and with a frictional behaviour tangential to the surfaces. The coefficient of friction between the steel and the timber was set to 0.4, and the penalty friction formulation was used.
A static general step was used in numerical simulations with Abaqus and with non-linear geometric effects toggled on. The increment was controlled to give curves without significant leaps and to apply the load in reasonably small steps.
The load displacement curves were defined based on displacement at the top edges of the plate and the hole to thereby measure displacement in the same location as the transducers used in the experiments.
For areas with significant tensile stress concentration, a linear elastic stress check based on beam theory was performed, namely by isolating the area of interest (e.g. a single lamination) and using a free body cut to find the forces and moment acting on the cut section with the highest stresses. Those values were subsequently used to determine stresses using Navier's equation.

3 RESULTS AND DISCUSSION

The load capacity of the studied connection in panels 120 mm thick is shown in Figure 6. The results reveal variation in load capacity depending on the geometry of the connection. Nearly all of the tested specimens failed in shear. Both rolling shear failures (i.e. at the bonded area between two adjacent laminations) and planar shear failure (i.e. with a crack parallel to the grain in laminations oriented perpendicularly to the direction of the applied load) were observed (Figure 2). However, it remains unclear which of the two shear failures occurred first.

Figure 2: *Failure mode of a type 1 specimen. The pictures show typical failure modes observed in most of the tested specimens. Both rolling shear in the outer horizontal laminations (upper picture) and longitudinal shear in the two internal vertical laminations (lower picture) can be seen*

https://doi.org/10.52202/069179-0158

The way in which the load is transferred from the openings where the anchoring plates are placed to the surrounding structure can be explained by the simplified model shown in Figure 3.

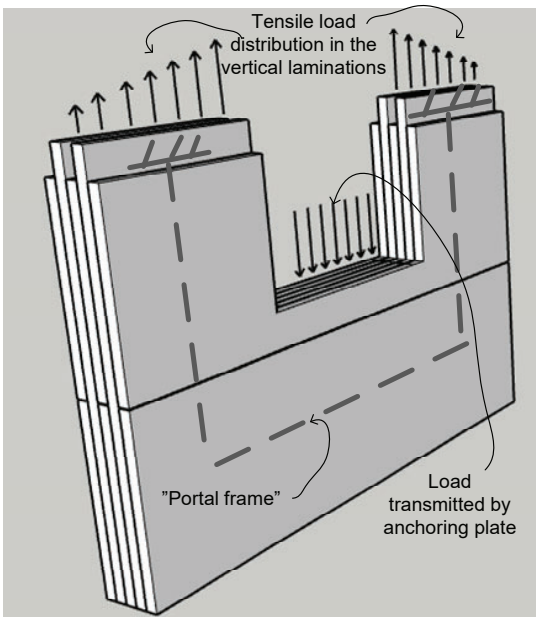

Figure 3: *Simplified model showing how the load is transmitted from the point of its application to the surrounding structure*

The part of the connection shown in Figure 3 suggests that the connection's structural behaviour is rather similar to that of an (upside-down) portal frame loaded with a distributed load at mid-span and rotationally restrained at the bases of the two frame columns. At the column bases, the bending moment and axial force generate a distribution of the reaction forces (virtually taken only by the vertical laminations) similar to that shown in the figure.

During loading, the portal frame is subjected to axial forces, shear forces and the bending moment. Those actions are most prevalently borne by the laminations of the portal frame with the grain parallel to the major stresses. For example, regarding the bending moment action in the frame, it will essentially be resisted by lamination 4 in the rafter part of the frame and by lamination 1 in the columns (Figure 4).

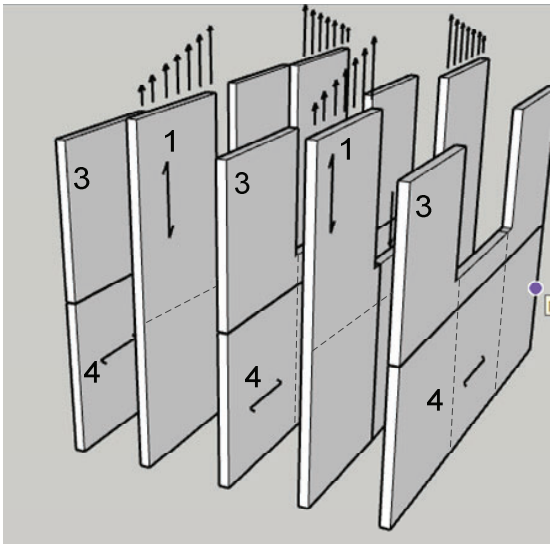

Figure 4: *Exploded sketch of the model shown in Figure 3. Laminations 3 and 4 have the grain in the direction perpendicular to the applied load, whereas Lamination 1's is in the direction parallel to the applied load*

However, because the vertical and horizontal laminations are bonded together, the bending moments and the consequent bending deformations in the load-bearing laminations are restrained by the cross-laminations. That dynamic generates torsional (shear) stresses at the bonded area between two adjacent laminations that might lead to failure due to rolling shear.

Similar considerations apply to the shear force in the frame. When the shear is transferred from the rafter (i.e. lamination 4) to the column (i.e. lamination 1), aside from rolling shear at the bonded areas, planar shear also occurs in lamination 1 (i.e. vertical shear) and in lamination 4 (i.e. horizontal shear) due to the moment gradient.

Finite element simulations revealed especially high shear stresses in all analysed specimens for loads close to the failure load. For example, for specimen type 1, the rolling shear and planar shear stresses at failure load are shown in Figure 5.

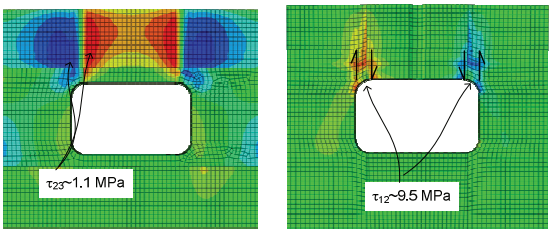

Figure 5: *Left: Rolling shear in outer horizontal lamination at failure load. Right: In-plane longitudinal shear in longitudinal lamination at failure load*

https://doi.org/10.52202/069179-0158

As shown in the analyses, shear stresses close to shear strengths are achieved for both rolling and planar shear, respectively.
In some of the sample with higher shear strength (i.e. specimens with larger DY), local bearing failure under the steel anchoring plate could be observed as well.
Our analysis of the results of laboratory tests suggests that the lateral distance, DX, within the tested range of 90 mm to 238 mm, had very little influence on the load-bearing capacity of the connection (Figure 6).

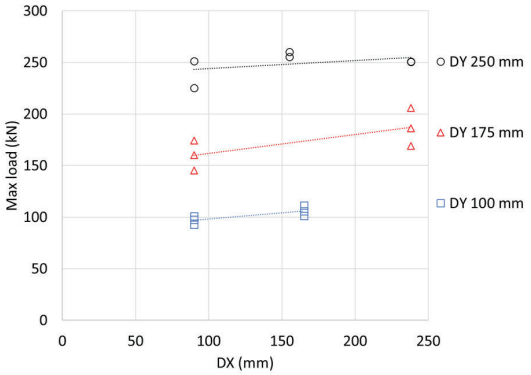

Figure 6: *Load capacity of the different tested specimens as a function of DX*

By contrast, there was also a clear increase in load-carrying capacity as the distance increased between the outer part of the anchoring plate and the upper (or lower) part of the specimen, DY (Figure 7).

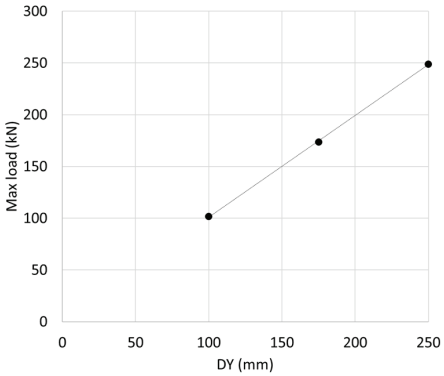

Figure 7: *Mean load capacity of the different tested specimens as a function of DY*

The stiffness of the connection was calculated as the ratio between the applied load and the local deformation measured underneath the anchoring plate. The maximum recorded local deformation for all of the tested specimens was generally small (i.e. approx. 1 mm), which led to very high axial stiffness of the connection. The stiffness was primarily influenced by the distance, DY, and to a lesser extent by DX. Moreover, the greater the distance, the lesser the influence of DX on the stiffness of the connection (Figure 8).

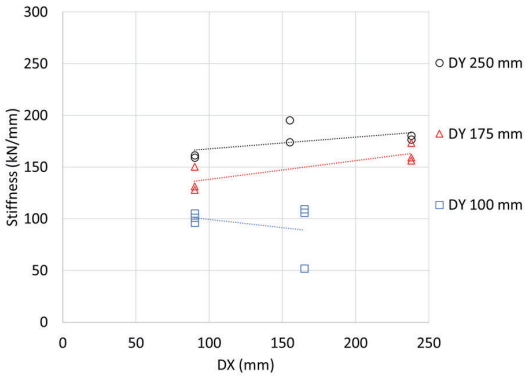

Figure 8: *Stiffness measured from local deformation.*

In terms of load displacement behaviour, FE analyses afforded highly accurate predictions. For example, a comparison of FE analysis and the laboratory results for one of the specimen groups is shown in Figure 9.

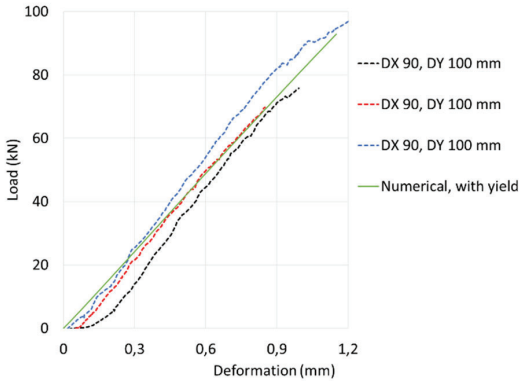

Figure 9: *Load versus local deformation for specimen type 1: comparison of experimental and FE results*

For the tested geometries, a pronounced linear relationship can be observed between the load-carrying capacity of the connection and the distance, DY. That condition, together with the fact that essentially all of the specimens failed in shear, lead to the formulation of a very simple verification model that was valid at least for a preliminary design of the connection within certain geometry boundaries. According to the model, the connection's capacity can be checked similarly to a check of the shear capacity of the rafter of a portal frame (Figure 10).

https://doi.org/10.52202/069179-0158

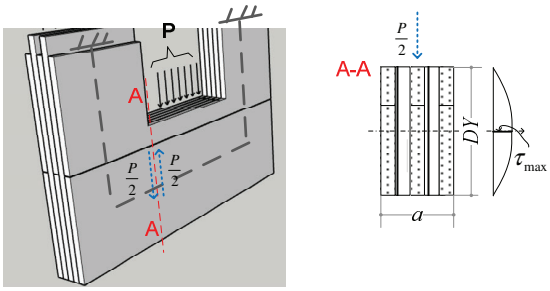

Figure 10: *Simplified verification model for the preliminary design of the proposed connection*

According to the model, the load carrying capacity, P, of the connection can be estimated as:

$$P = \frac{4}{3} \cdot a \cdot DY \cdot f_v \qquad \text{Eq 1}$$

in which a and DY are as explained in Figure 10, and f_v is the shear strength of the gross cross-section. For the tested specimens, the mean value of f_v was approximately 6.2 MPa. That relatively high value of shear strength, however, is suitable only for predictions of the realistic capacity of the connection. For a design situation, a lower shear strength value, presumably in the range of 3 to 4 MPa, is advisable.

4 CONCLUSIONS

The chief findings of our study were that:

- DX's influence on the load bearing capacity of the investigated connection is rather slight
- DY has significant influence on the load bearing capacity of the connection and
- Failure modes and corresponding failure loads are predictable for the geometries tested.

The novel structural connection demonstrates properties of strength and stiffness that are adequate for applications in connections between wall elements and between floor and ground foundations in multi-storey building. A single connection of this type can thus replace hundreds of conventional fasteners such as screws and nails.

ACKNOWLEDGEMENTS

Our research received financial support from the Kamprad Family Foundation (Ref. No. 20200013). We also wish to thank the Södra Skogsägarna forestry cooperative, especially Daniel Anderson and Kristoffer Segerholm, for the CLT used in the specimens.

REFERENCES

[1] Blomqvist, L., Honfi, D., Johansson, M., Ziethén, R., Crocetti, R., Norén, J.: Development of novel structural connections – Inspiration from furniture industry. In: Proceedings of the 2021 World Conference on Timber Engineering (WCTE), 2021.

[2] Basic, A., Amrllahu, K.: Korslimmat trä – styvhet vid belastning i planet. Student thesis (Degree project). Lund, LTH, 2018.

https://doi.org/10.52202/069179-0158